REVIEW

Turbulent drag reduction research at NASA Langley: Progress and Plans*

S. P. Wilkinson, J. B. Anders, B. S. Lazos, and D. M. Bushnell
NASA Langley Research Center, Hampton, VA 23665, USA

Received December 1987

The paper summarizes the status of the ongoing NASA Langley research program in the area of turbulent skin friction reduction. The discussion is organized under the general headings of (a) approaches which work, (b) approaches which may work, and (c) approaches which evidently do not work, although many of the latter provide turbulence alteration and control (but not net drag reduction). Riblets are currently in the flight application stage, whereas large-eddy breakup devices are still under laboratory study, particularly in regard to device drag minimization and performance at flight device Reynolds numbers. A new generation of wall region approaches offers promise, but the research is still in an early stage.

Keywords: turbulent drag reduction; turbulent boundary layer

Introduction

The impetus for turbulent drag reduction research is both tremendous and obvious. A large proportion of the energy expenditure for all types of transportation (air, sea, land) and for many industrial and propulsion processes is simply to overcome turbulent skin friction. The payoff from invention and development of successful approaches can conservatively be estimated in the billions, irrespective of which country's currency one considers. The approaches of research choice prior to the late 1970s involved either laminar flow control (LFC), which had fairly severe limitations as to application (surface finish/unit Reynolds number, disturbance environment, etc.), or techniques to alter the average flow/drag directly such as (a) wetted area minimization, (b) reduced roughness, (c) use of a "Stratford closure" (adverse pressure gradient), (d) mass injection, and (e) bubbles to reduce the average near-wall density in water.[1] An exception was the use of polymers to affect, in an unknown manner, the turbulence field directly.

Following an unsuccessful four-year campaign to apply "complaint walls" to the case of airflow (1972–1976, Ref. 2), and recognizing the extensive contemporary research on wall turbulence structure, the NASA Langley drag-reduction effort turned toward a more overt invention-orientated mode of operation in 1976 and posed the following question: Does a smooth flat surface really provide the lowest net drag or are there other (nonplanar) surfaces which could interfere with various facets of the wall turbulence structure and provide a net drag reduction? By 1978 two new approaches, still under active study, had arisen from this effort: (a) riblets,[3] and (b) large-eddy breakup devices.[4,5] The latter was developed in cooperation with the IIT group (H. Nagib) under grant. Along with these two approaches, which are still the current "front runners" among the passive, nonplanar techniques, many other approaches were tried and discarded.

* The paper was first presented at an international conference on "Turbulent Drag Reduction by Passive Means" organized by the Royal Aeronautical Society and held at the Society's headquarters in London 15–17 September 1987. It is here reprinted by permission of the Society. The complete Proceedings of the Conference are available from The Royal Aeronautical Society, 4 Hamilton Place, London W1V 0BQ, UK.

The Langley effort in turbulent drag reduction is still continuing and involves research across the spectrum from application-orientated studies to fundamental physics and flow phenomena investigations on a current total of nine techniques. The present paper summarizes the status of this research and includes a brief section documenting the various techniques which were studied over the last decade and found wanting in some way.

It should be noted that large-scale application of viscous drag reduction techniques to aircraft generally requires concomitant decreases in drag-due-to-lift to allow efficient operation and accrual of the full benefits. Therefore, NASA Langley has a companion research effort in the drag-due-to-lift reduction area including swept-back tapered tips, tip blowing, serrated trailing edges, tip turbines, and other devices, many of which were suggested by morphological studies of Nektons and Avians.

Approaches which work

Riblets

Of all the nonplanar surface approaches to turbulent viscous drag reduction, riblets are the best established with little if any remaining doubt regarding their effectiveness. The following discussion reviews low-speed experimental and theoretical riblet studies from Langley and other institutions with emphasis on the fluid mechanical mechanisms involved. The Langley study of thin-element riblets is dealt with at length. A brief update on riblet flight tests and other riblet applications is also presented.

The main thrust of the initial Langley riblet research was to verify riblet drag reduction and optimize its level.[3,6–9] This effort culminated in the selection of a symmetric v-groove as the optimal design ($h^+ = s^+ \simeq 15$, 8% drag reduction[7]). Independent studies have also verified drag reduction with riblets.[10–24] Other significant findings from the Langley work reported during this period were that the physical riblet dimensions for drag reduction scaled in wall variables; v-groove design was insensitive to yaw angles up to $\pm 15°$; sharp-peaked riblets appear to perform better than rounded peaks; riblets appear to function in moderate adverse and favorable pressure gradients;[25] and the Reynolds analogy factor is 30% higher for a v-groove riblet than for a smooth flat plate.[26] A less appreciated finding implicit in the above work is that requirements for *any* drag reduction as opposed to *optimal* drag reduction are not particularly severe. The data clearly show that many riblet cross-sectional designs with height less than about 15 wall units and spacing less than 140 (based on new data below) can provide some measure of drag reduction. This is an important observation in terms of possible drag-reduction mechanisms since such mechanisms cannot be linked exclusively to particular geometric details (e.g., peak sharpness, slope of groove side walls, etc.).

Concurrent with the Langley work, several more specific and detailed studies of the symmetric v-groove design were conducted at the University of Maryland (under Langley grant, Ref. 14) and Lockheed-Georgia[15] to determine the physical process by which riblets reduce drag. Both studies support a viscous effect whereby drag reduction due to slow, quiescent flow in the riblet valleys (which places a slip boundary condition upon the turbulence production process) outweighs the increase in drag due to increased wetted area and higher relative drag on the riblet peak regions.

Others find a more substantial role for the influence of riblets upon coherent structures. In work conducted at Lehigh University[23] and British Maritime[27] the upwelling between counter-rotating wall vortices and lateral movement of such vortices is seen as being restrained by the riblet peaks with a concomitant reduction in bursting activity and drag. Work conducted at Michigan State University[28] suggests that the thickened sublayer due to the riblets may reduce the tendency of typical eddies to initiate bursting. A numerical effort at Lockheed-Georgia[29] predicts 20% drag reduction for the optimal v-groove design employing a unidirectional algebraic Reynolds-stress turbulence model. The computations show formation of streamwise vortices along the v-groove sides which are essential for the calculated drag reduction. The very small lateral wavelength of these vortices ($\lambda_z^+ \sim 16$) and their large vertical extent ($y^+ \sim 50$) suggests, however, that they may not be physically realizable and that the turbulence model is not correct.

A novel approach to riblet analysis has been developed at DFVLR-Berlin[10] in which conformal mapping is used to map the linear sublayer profile of a smooth flat plate onto a variety of sublayer-scale riblet surfaces. The results show that riblets cause substantial reduction of shear stress within the riblet

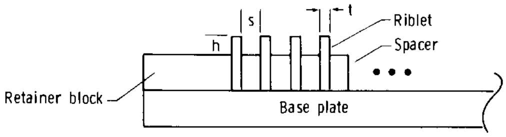

Figure 1 Thin-element array model assembly

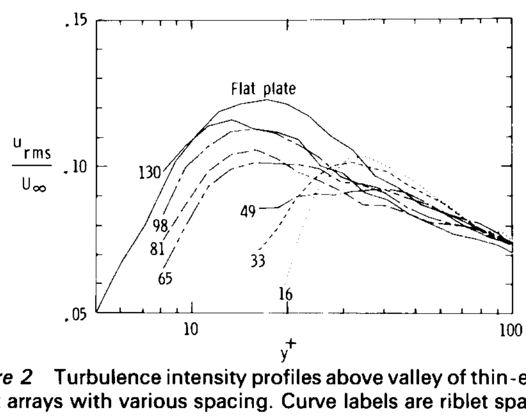

Figure 2 Turbulence intensity profiles above valley of thin-element riblet arrays with various spacing. Curve labels are riblet spacing in approximate wall units

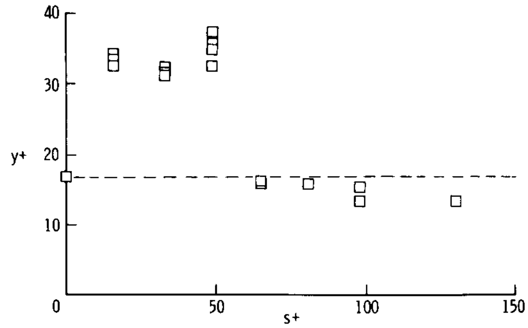

Figure 3 Location of peak in turbulence intensity profiles above riblet valley. Dashed line is location of peak for reference smooth flat plate

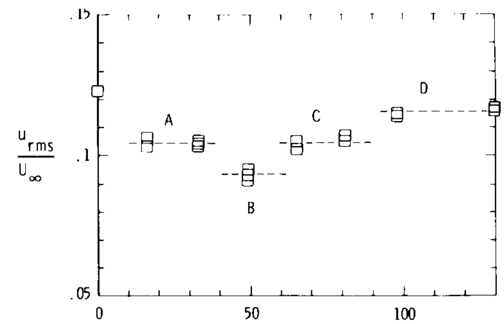

Figure 4 Maximum value of turbulence intensity above riblet valley for various riblet spacings

valley and increase shear stresses near the peak. While the technique cannot predict absolute or even relative shear stress among various models, it agrees qualitatively with the Maryland measurements[14] and suggests that the primary drag reduction mechanism is a favorable redistribution of shear stress due to quiescent flow.

Langley thin-element study

A recent Langley study of thin-element riblets[24] has helped to sort out riblet physics and tends to substantiate the theory that riblet drag reduction is probably not due primarily to alteration of turbulence production.

Figure 1 shows the thin-element riblet geometry and model construction technique. This particular design was chosen because it allows fairly easy independent variation of riblet height and spacing. Both hot wire and direct drag data were acquired for several series of thin-element models. Figure 2 shows normal profiles of streamwise turbulence intensity taken on the centerline of the riblet grooves with various physical spacing but constant physical height. To help elucidate the behavior of the curves in Figure 2, two cross-plots are provided in Figures 3 and 4. Figure 3 shows the vertical location of the peak in the intensity profiles in wall units ($y^+ = yu_\tau/\nu$ = height, u_τ = friction velocity, ν = kinematic viscosity) and Figure 4 shows the peak intensity magnitude for each curve. The striking feature of Figure 3 is the discontinuity in the region $50 < s^+ < 65$. For riblet spacings greater than $s^+ = 65$, the peak intensity location is approximately that of the smooth flat reference plate whereas for $s^+ < 50$, the peak intensity location is displaced upward by approximately the riblet height. The significance of this data is that it shows the existence of a minimum value of riblet spacing below which certain turbulent motions are excluded from the groove region. The fact that this spacing is in the range of roughly one-half the average spanwise wavelength of wall streaks strongly suggests that wall streaks (or those

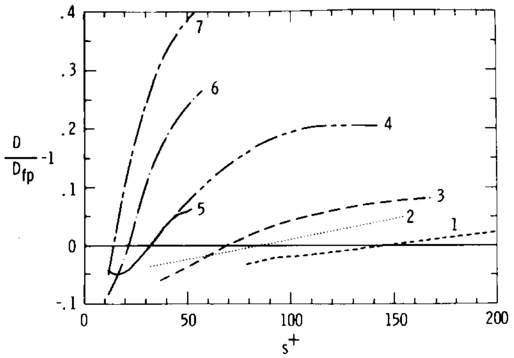

Figure 5 Direct drag for thin-element riblet models listed in Table 1

Table 1 Thin-element riblet array model dimensions

Model	*h* (mm)	*s* (mm)	Aspect ratio
1	0.25	3.56	0.07
2	0.25	1.63	0.15
3	0.33	2.03	0.16
4	0.51	1.63	0.31
5	0.25	0.64	0.80
6	0.51	0.64	0.80
7	0.64	0.64	1.00

All models: riblet thickness 0.051 mm.

turbulent motions which produce the wall streaks) are accommodated within the thin-element channels only for riblet spacings greater than 50 wall units. Figure 4 shows that the intensity is at minimum at $s^+ = 50$ with an indication of discrete shifts in intensity levels at other spacings. The behavior may be related to accommodation between the riblets of coherent turbulent structures of discrete spanwise length scales either individually or in pairs. Sandborn and Chien[30] conducted a study of the effect of closely spaced boundary layer fins similar to the thin-element riblets but with a fin height of $0.27\,\delta$ and a length of $0.49\,\delta$ where δ is the boundary layer thickness of the undisturbed flow. The fins produced maximum downstream skin friction reduction or a spacing of approximately 60 wall units, with less reduction for smaller and larger fin spacings. Figure 4 suggests similar behavior for the thin-element riblets.

Based on Figures 4 and 5, one might expect similar discontinuous behavior in direct drag data, especially around $s^+ = 50$. This has not been observed in any previous experiments, nor is it observed in the present drag data. Figure 5 is a plot of drag of thin-element riblet models relative to a smooth flat reference plate corresponding to model parameters listed in Table 1. There is no discontinuous behavior in either the drag reduction or drag increase regions of the plot for any of the models. One must conclude that the "discontinuity" depicted in Figure 3 has at most only second-order influence on total model drag.

Mean velocity and turbulence intensity data for a single, isolated thin-element riblet are shown in Figures 6 and 7 and indicate waveform signatures which are consistent with a pair of counterrotating vortices along the riblet. It is significant that the spanwise wavelength of the pattern in Figure 6 ($\lambda_z^+ = 130$) is of the same order as the commonly quoted $\lambda_z^+ = 100$ for average wall streak spacing. A search of the literature shows that similar vortices have been observed in previous studies. The earliest data in this regard is the 1966 Stanford[31] work on widely spaced rectangular-shaped riblets in a water channel flow in which longitudinal vortices were observed to form along the riblets. Somewhat related work was conducted at Kyoto University[32] where large-scale streamwise cellular currents were found along very widely spaced rectangular riblets in a shallow open-channel flow.

The vortices believed to be represented in Figures 6 and 7 should also be present along widely spaced riblets (i.e., $s^+ > 50$). The effect of the presence of the vortices, however, on drag is uncertain. Drag reduction for the thin-element riblets persists out to $s^+ = 140$ as shown in Figure 5 and may result from aligning and separating the vortices. The drag reduction in this region could also be due, however, to the 90° quiescent riblet corners which are present at any spacing. There is no conclusive evidence, therefore, that anchoring or separating vortex pairs with riblets produces drag reduction.

A further lesson learned from Figure 5 is the nearly monotonic influence of riblet aspect ratio (h/s) on drag. The models are numbered in order of increasing aspect ratio and it is clear from Figure 5 that aspect ratio has a first-order influence on the rate of drag change with velocity. The tendency of the curves to roll off as s^+ increases is most likely due to boundary layer thinning with increasing stream velocity.

The overall conclusion to be drawn from the thin-element study is that drag reduction is apparently due to relatively quiescent flow in the riblet grooves. This quiescent flow is maintained by a mismatch between the scale of the energetic structures which exist near the wall and the riblet spacing. While there is good evidence of interaction between thin-element riblets and turbulence (i.e., streamwise vortex formation) the resulting effect on total drag is, at best, second order.

Riblet flight tests

In the past year, riblet flight tests employing 3M vinyl riblet film at low transonic speeds ($M \simeq 0.7$) have been conducted by Langley on a Lear jet. Tests involved both pitot rake momentum measurements and several different local direct drag balances designed specifically for flight tests. Experimental data are

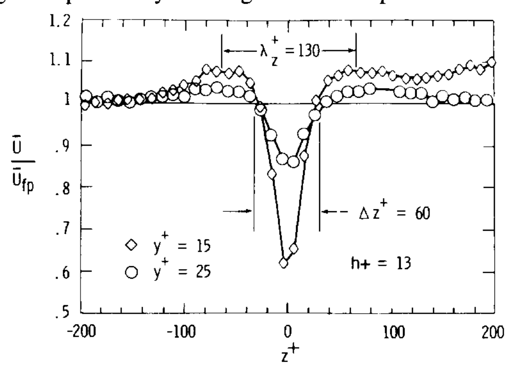

Figure 6 Mean spanwise velocity profiles above single, isolated thin-element riblet ($h^+ = 13$). Data normalized with reference smooth flat plate velocity at same y^+

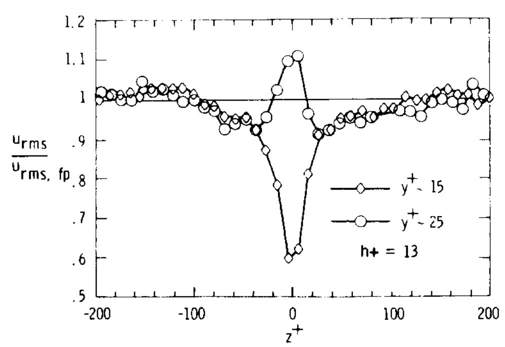

Figure 7 Spanwise turbulence intensity profiles above single, isolated thin element riblet ($h^+ = 13$). Data normalized with reference smooth flat plate intensity at same y^+

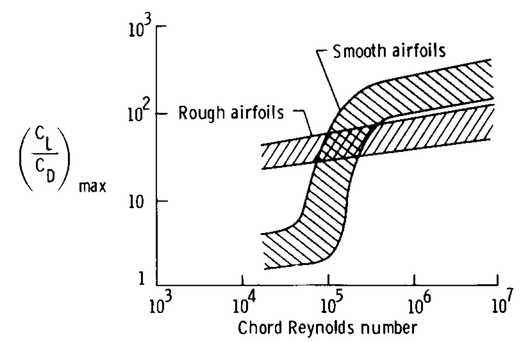

Figure 8 Low Reynolds number airfoil performance

currently being evaluated but it can generally be reported that the tests were successful and about what was expected in agreement with previous Boeing riblet drag reduction measurements on a T-23 airplane at Mach 0.7[13] based on pitot rake momentum data. Outstanding problems regarding successful application of riblets to aircraft are film porosity and particle adhesion.

Other riblet applications

A 1984 U.S. Summer Olympic rowing team (four-man with coxswain) employed 3M riblet film on the rowing shell and placed second in an event in which the United States had traditionally done poorly. Details are presented in Ref. 16. More recently, the U.S. America's Cup challenger employed 3M symmetric v-groove riblet film ($h=0.11$ mm, $s=0.11$ mm) over the submerged hull and achieved victory both intramurally and in competition with the New Zealand and Australian vessels. Other design changes concurrent with the film application, however, preclude definitive assessment of the riblets' performance alone.

LEBUs

Large-eddy breakup (LEBU) devices have been shown, in a number of careful low-speed experiments, to effect large skin friction reductions (peak reductions of the order of 30–40%) over long distances downstream (20% average C_f reduction over 100–150 boundary-layer thickness). It is clear from the long relaxation times that LEBUs do modify the large-eddy structure of the turbulent boundary layer inhibiting in some unspecified way the Reynolds stress production near the wall. The skin friction reduction effectiveness of large-eddy structure changes was first demonstrated by Yajnik and Ancharya[33] using screen fences. Later work at IIT[34–36] and NASA Langley[37–40] showed that minimizing the device drag using thin ribbonlike devices produced net reductions (i.e., C_f reductions larger than device drag) ranging from 5–15%. Airfoil-shaped devices, required for greater structural rigidity at higher speeds, have also been shown to produce up to 7% net drag reductions.[41]

Several mechanisms have been proposed to explain LEBU drag-reduction performance. These include (1) the blocking effect of the embedded, impervious surface, (2) the momentum deficit of the device wake, (3) turbulence distortion from the mean flow alteration, (4) vortex "unwinding" from the opposite-sense, starting vortex shed from the device trailing edge (produced by the upstream approach of large vortical structures), (5) the downstream influence of control vortices shed from the device trailing edge, and (6) macromovement of momentum away from the surface due to device circulation. All of these mechanisms may contribute to some degree to the drag-reduction effectiveness of the devices but the dominant mechanism(s) are still in doubt.

A persistent problem in all experiments to date (now including more than 40 institutions worldwide) has been the extreme variability of results not only from lab to lab, but even within the same laboratory. A number of causes have contributed to this disagreement, such as (1) testing in non-equilibrium or "special" boundary layers, (2) skin friction measurement errors, and (3) variations in device geometry. Known sensitivities include device thickness, height above the surface, angle of attack, single or tandem arrangements and device vibration induced by the flow. The overriding cause of result variability seems to stem from the universally low-chord Reynolds numbers of all tests to date. Anders[42] examined LEBUs from the viewpoint of low Reynolds number airfoils and concluded that the devices are extremely sensitive to the disturbance environment (the oncoming turbulent boundary layer) and that device imperfections can compound this sensitivity, much as in the case of low Reynolds number airfoil testing.[43] Figure 8 (from Ref. 44) shows $(L/D)_{max}$ for smooth airfoils can vary by orders of magnitude in the chord Reynolds number range from 50,000 to 200,000, which corresponds to the range of the bulk of current LEBU experiments. The extreme sensitivity illustrated in Figure 8 is due to separation/transition/reattachment of the initially laminar device boundary layer and can lead to large-scale spanwise flow structures downstream.[45] In the case of LEBUs, the highly unsteady, incoming turbulent boundary layer with a plethora of three-dimensional disturbance scales induces a three-dimensional, time-varying angle-of-attack variation along the span of the device producing upwash/downwash effects on the large-eddy structure. The downstream result of this complicated picture was documented in Ref. 42 where small systematic modifications to device geometry were shown to produce dramatic downstream results. Figures 9 and 10 from Ref. 42 show that much of the mean three-dimensional structure that develops downstream of LEBU devices is directly attributable to spanwise microgeometry variations in the devices themselves; specifically the trailing-edge shape/thickness. It was also shown in Ref. 42 that airfoil-shaped devices have this same sensitivity to trailing-edge shape/thickness and that unsteady, laminar separation was occurring over most of the airfoil most of the time.

The importance of the trailing-edge region to drag reduction in low Reynolds number flows has been further investigated in Ref. 46 where acoustic excitation of the LEBU trailing edge, when phased with the oncoming turbulent eddies, was shown to increase downstream skin-friction reductions appreciably. This effect may be due to a modification of the shed vorticity from the LEBU, or simply a transition/reattachment trigger for

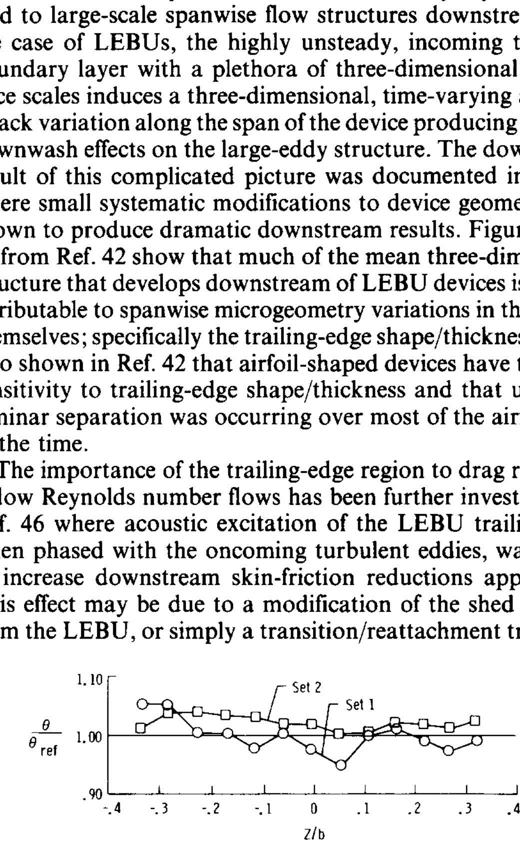

Figure 9 Spanwise variation of momentum thickness at $\Delta x/\delta=108$, tandem NACA 009 airfoils, $\Delta s/\delta_0=5$, $h/\delta_0=0.8$

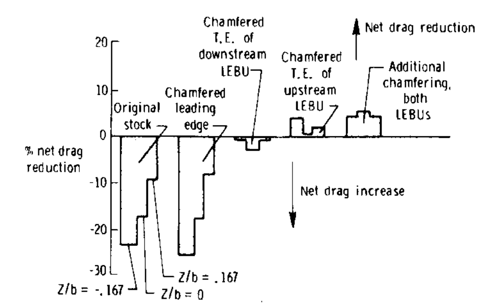

Figure 10 Net drag reduction with device leading- and trailing-edge microgeometry, thin-element set 2

the unsteady, separated device boundary layer. In any event, it is clear that, as in the case of conventional low-Reynolds-number airfoil testing, viscous effects dominate the flow field over the devices.

Computational results using rapid distortion theory[47] have indicated that positive lift (away from the wall) is beneficial in reducing fluctuations of the vertical velocity component downstream, indicating that cambered lifting devices may be more effective. This result supports the experimental data showing thin-ribbon devices at a small (less than 1°) positive angle-of-attack produce larger C_f reductions, but that larger angles dramatically increase device drag effectively negating any net reductions.

The conclusions from this discussion seems clear: Low Reynolds number effects are present in all experimental results presented thus far, and these effects are responsible for some of the extreme LEBU sensivities noted by researchers. The problem may be moot since any application of LEBU drag reduction to a flight vehicle will result in device chord Reynolds numbers of 300,000–500,000 and at these Reynolds numbers the sensitivity and variability of results should be somewhat less. Higher Reynolds number results are urgently needed to fully assess the drag reduction potential of LEBU devices.

The only published high-chord Reynolds number results on LEBU drag reduction have been those of Bertelrud.[48] In a flight experiment where LEBU devices were mounted on the swept wing of a Swedish fighter, he found average skin friction reductions of up to 20% over 100 boundary layer thicknesses downstream at Mach 0.8. Net drag reduction was not measured in this experiment and it is unlikely that any was obtained because of the thick, crudely shaped airfoil devices used. It is encouraging to note, however, that the LEBU drag reduction mechanism(s) worked well at transonic speeds, with up to 40° of device sweep. Net reductions will require low drag, shock-free devices and computational work at NASA Langley has produced several promising candidate airfoils that perform well in the presence of a nearby surface. Transonic testing of these candidate airfoils in a small scale facility is currently underway in preparation for a larger scale test in the Langley 7′ × 10′ tunnel on a 30′ cylinder model. Results from these tests will be used to design airfoil LEBUs for a full-scale flight experiment on the fuselage of a Boeing 737 transport early in 1988. Concurrent with these studies, an experiment is being conducted in the Naval Underwater Systems Center tow tank at Langley. In this test, LEBU airfoils mounted on an axisymmetric body are being evaluated for drag reduction effectiveness at chord Reynolds numbers from 150,000 to 400,000, essentially duplicating the flight Reynolds number regime but in incompressible flow, thus avoiding the shock/compressibility device drag issue.

There are a number of intriguing possible applications for large-eddy breakup devices aside from drag reduction. These include (1) lower self-noise for hydrodynamic and aerodynamic vehicles, (2) reduction of noise from turbulence-propeller interactions for rear propulsors, and (3) reduced "jitter" of laser beams transmitted through fuselage boundary layers. Also, LEBU-modified boundary layers have shown a significantly reduced intermittency and a reduced overall boundary layer thickness thus enhancing the possibilities for effective slot suction removal/relaminarization.

Approaches which may work

Two-stage control

This section presents progress and plans for a number of candidate drag-reduction techniques which have not yet proven fruitful. The lack of positive results, however, is considered as being due more to low device efficiency (which may be improvable) along with an incomplete theory of turbulence rather than to any currently identifiable fundamental flaw in the concepts. The techniques for which new data are presented include two-stage control, compound riblets and three-dimensional riblets. Separation control, eddy substitution and curvature effects are discussed although new data are not available.

While drag reduction with passive straight riblets remains in the 5–10% range, the observation that widely spaced riblets generate longitudinal vortices has led to the two-stage control approach. The idea is to actively modify (with suction or blowing) widely spaced riblet vortices as a possible means of controlling turbulence production. The concept is currently being developed at Notre Dame and USC[49] as well as at Langley. The Notre Dame/USC study has shown that it is possible to eliminate artificially generated vortex pairs in a laminar boundary layer with selective streamwise slot suction. Without suction, the same vortex pairs exhibit bursting behavior similar to that believed to take place in a turbulent flow. Some reduction in bursting in a turbulent boundary layer is also observed by applying continuous high flow rate slot suction. None of the two-stage control research to date has shown any evidence of ability to control turbulence with the exceedingly small control inputs required to effect net reductions. Only a few techniques have been tried, however, and it is too early to rule out the method altogether.

The major problem with suction as a control agent is that it contributes directly to total drag by momentum transfer from suction mass flow to the test model. (A similar problem exists with blowing when viewed from a system perspective.) The suction level at which drag due to suction mass momentum transfer becomes comparable to viscous skin friction for the unaspirated case is very small ($c_{q,\mathrm{avg}} \sim 10^{-3}$). An average coefficient on the order of $c_{q,\mathrm{avg}} = 10^{-4}$, therefore, appears to be necessary before a viable drag-reduction system can be envisioned. The Notre Dame/USC study estimates that the average suction requirement for artificial vortex control in laminar flow can be as low as $c_{q,\mathrm{avg}} = 6 \times 10^{-4}$ when suction is applied very sparingly, both spatially and temporally. Although this is probably still too large for net drag reduction, further optimization may be possible. The approach presented previously was used to design a simple aspirated riblet model in which continuous suction was applied to the peak region of widely spaced riblets. The aim was to determine what effect low level suction ($10^{-4} < c_{q,\mathrm{avg}} < 10^{-3}$) had on net drag and if such effect could be attributed to the stabilizing influence of suction on riblet vortices. The model is illustrated in Figure 11 with dimensions in Table 2. Each suction riblet actually consisted of two riblets with a small space between them through which suction or blowing could be applied. In terms of wall units, the model was designed for a spacing of nominally $s^+ = 100$ and height, $h^+ = 15$ to enable a vortex pair to exist within each

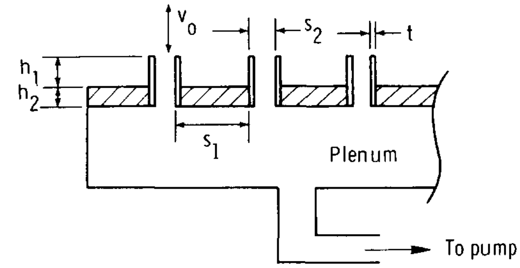

Figure 11(a) Widely spaced riblets with peak suction or blowing: cross-sectional view

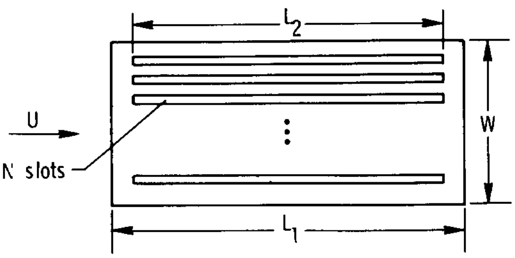

Figure 11(b) Widely spaced riblets with peak suction or blowing: plan view

Table 2 Dimensions for widely spaced riblet model with suction or blowing (Figure 11)

h_1	0.5
h_2	12.2
s_1	3.2
s_2	0.2
t	0.05
L_1	305
L_2	279
W	279
N	77

All dimensions in millimeters.

riblet channel. The amount of open area was 5.1% of the total plan surface area. A smooth porous plate with small discrete perforations was attached to the same plenum chamber as the riblet model and provided reference data. The diameter of the perforations was $d=0.064$ mm ($d^+ \sim 2$) and the spacing $L=$ 0.64 mm ($L^+ \sim 20$) in a square array. Plate thickness was 0.64 mm and open area 0.78%.

Drag was measured in the Langley 7 x 11-inch low-speed wind tunnel with a direct drag balance. Suction was applied through a calibrated water seal to eliminate drag balance errors due to mechanical attachment of a suction line. A simple plumbing change allowed blowing to be applied to the riblet peaks. Direct drag data is shown in Figures 12 and 13. (There was no significant difference between drag on a smooth impervious flat plate and drag on the perforated surface in the absence of suction or blowing.) Figure 12 shows absolute C_d level at a fixed stream velocity of 10 m/s ($Re_\theta \sim 1000$) for both suction and blowing. The data fairings are second-order curve fits. The average suction/blowing coefficient is defined as the total volumetric flow rate divided by the product of total plan (i.e., projected) area and free-stream velocity. As can be seen at $c_{q,avg}=0$ the riblet model had 10% higher drag than the reference perforated surface (or smooth impervious plate). This is not surprising in view of the relatively large width of the dual riblets ($w^+=10$). As the suction or blowing rate is increased, the total drag rises or falls as indicated. The behavior of the riblet surface relative to the reference perforated surface is better illustrated when the data is normalized with the drag at $c_{q,avg}=0$ as shown in Figure 13. It is evident that there is no significant difference between suction through a smooth porous surface and suction applied to the riblet peaks. If the suction reduces bursting more for the riblet case than for the reference case, that rate of increase of drag with c_q should also be less. This is clearly not the case for the current models, at least within the scatter of the data.

For the case of riblet peak blowing, Figure 13 shows that the riblet surface performs poorly relative to the smooth porous surface. The most evident reason for this behavior is that flow through the smooth porous surface acts directly to alleviate du/dy at the wall whereas the riblets inject fluid less productively at a higher location in the boundary layer. There is reason to expect that peak blowing would promote turbulent bursting and increase drag but the data indicate that the primary effect of blowing is to reduce mean shear stress either at the wall or at the riblet peak.

The overall conclusion to be drawn from the riblet peak suction/blowing experiment in that there is no clear evidence that continuous streamwise suction or blowing uniquely affects riblet vortex bursting in such fashion as to either decrease or increase drag at the c_q levels tested. It is possible that the current model may be "wasting" significant suction on nonproductive flow at streamwise locations where the flow is relatively quiescent (i.e., not bursting).

Compound and three-dimensional riblets

In an effort to improve riblet drag reduction passively through alternative mechanisms (i.e., nonviscous) direct drags of a variety of compound and three-dimensional (3D) designs have been measured in the Langley 7 x 11-inch tunnel. A compound riblet is defined as one which allows spanwise variation in height, spacing, or cross-sectional shape while maintaining streamwise uniformity. Earlier Langley work on compound riblets includes the notched peak v-groove[6] which showed an extended drag reduction range. A three-dimensional riblet model allows variation in height, spacing, and shape in both spanwise and streamwise directions. Although it is generally agreed that quiescent riblet groove flow is the primary cause of drag reduction, interactions between riblets and turbulent structures are readily observable (e.g., Ref. 24). Therefore, an additional goal of the compound and three-dimensional riblet experiments

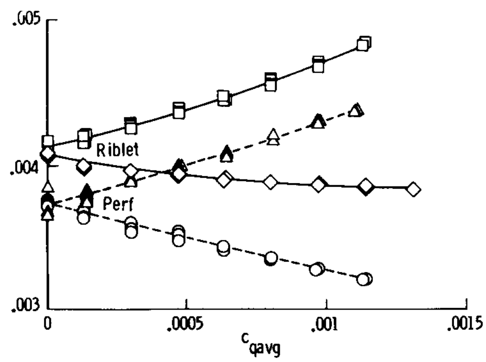

Figure 12 Direct drag for widely spaced riblet and smooth perforated plate with suction or blowing: symbols: square = riblet suction; triangle = pref. plate suction; diamond = riblet blowing; circle = perf. plate blowing

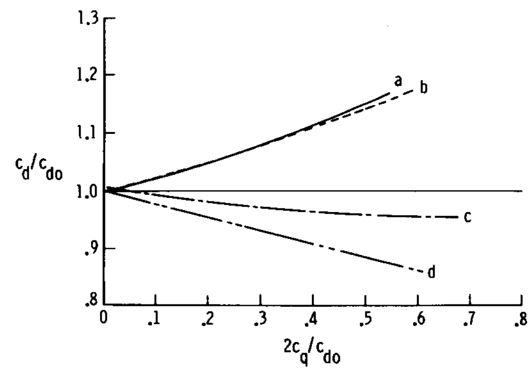

Figure 13 Normalized direct drag for widely spaced riblet and smooth perforated plate: labels: a = riblet suction; b = perf. plate suction; c = riblet blowing; d = perf. plate blowing

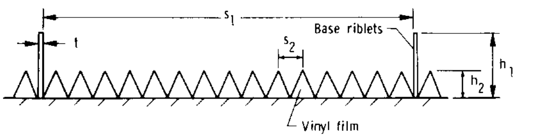

Figure 14 Compound riblet model C1: $s_1=2.03$, $h_1=0.33$, $s_2=0.15$, $h_2=0.15$, $t=0.051$ (all millimeters)

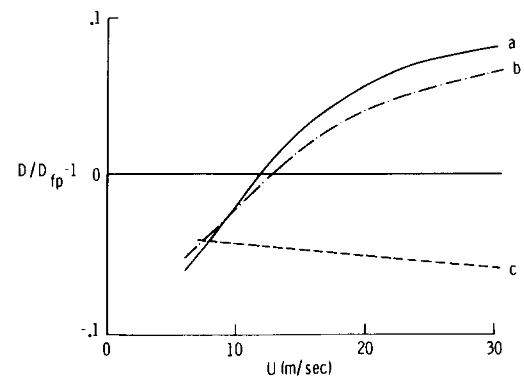

Figure 15 Direct drag for model C1: labels: a = base riblets alone, b = combined base and vinyl film riblets, c = vinyl film riblets alone)

was to further investigate whether observed changes in drag due to various riblet designs could be associated with interactions between riblets and the turbulent flow.

The first compound riblet model (model C1) consisted of conventional v-grooves (3M vinyl film) situated between higher, more widely spaced thin-element riblets as illustrated in Figure 14. Both configurations alone were known to reduce drag. The closely spaced v-grooves function primarily through their ability to create a low drag, quiescent groove flow. There is evidence that the widely spaced thin-element design causes formation of streamwise vortices along their peaks.[24] If drag reduction for the widely spaced thin elements is due to such vortices via turbulence alteration, the possiblity exists that the combined effect of the two types of riblets might be additive. Direct drag data for the two individual models and the compound model are shown in Figure 15. It is clear that the levels are *not* additive indicating that the individual models most likely reduce drag by the same mechanism. The high thin elements (base riblets) apparently assume control of model drag by introducing wetted surface area in relatively high mean velocity regions away from the wall. The compound model shows a slower rate of drag increase than the thin-element model alone over most of the s^+ range shown. This can be attributed to the decreased effective aspect ratio of the compound model ($h/s=0.13$) relative to the thin-element model alone ($h/s=0.16$) as discussed with regard to Figure 5. Overall, model C1 does not improve drag reduction nor is their any clear evidence that the compound design promotes a mode of drag reduction (or increase) that can be attributed to riblet vortices which are believed to occur along the high, thin-element riblets.

The second compound model (model C2) employed two v-grooves of widely different aspect ratios (0.07 and 1) as illustrated in Figure 16. This model was based on incorrect initial data which showed that the low aspect ratio v-groove provided a uniform 4% drag reduction. Based on this incorrect data, the rationale for model design was similar to model C1, i.e., determine if the drag-reduction levels are additive. As shown in Figure 17, however, drag for the low aspect ratio v-groove was not significantly different from the reference smooth flat plate. Based on this data, enhanced performance of the compound model would not be expected. As shown, the compound model actually may have degraded performance of the closely spaced v-grooves alone.

The first of the three-dimensional models (model 3D1) was an attempt to improve performance of the best thin-element model (Figure 5, model 6). The rationale was to reduce the wetted surface area of the riblets by making the riblets periodic in the streamwise direction as illustrated in Figure 18. The wetted surface area ratio, A/A_{fp}, was 1.89 for the three-dimensional model compared to 2.6 for thin-element model 6. The streamwise wavelength of the periodic riblets was approximately 500 wall units roughly corresponding to the length of turbulent structures in the wall region. Direct drag data is shown in Figure 19 for models 3D1 and 6. As can be seen, the streamwise periodicity degraded performance substantially. The increased drag may be attributable to several factors, most likely increased frontal area and possibly vortex generation by the elements.

The second three-dimensional riblet model (3D2) was an attempt to improve model C1 by making the high, widely spaced riblets periodic in the streamwise direction (i.e., reduce wetted area as in model 3D1). The model is illustrated in Figure 20. Note that thin-element riblets have been substituted for v-grooves in Figure 14. The relative height of the high, short riblet segments was adjustable on this model. Data is presented in Figure 21. As can be seen, the only effect of the three-dimensional widely spaced riblet segments is to degrade performance. The increase in drag is also roughly proportional to the

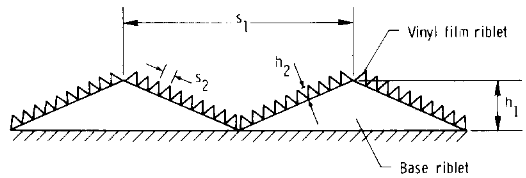

Figure 16 Compound riblet model C2: $s_1=3.15$, $h_1=0.25$, $s_2=0.15$, $h_2=0.15$ (all millimeters)

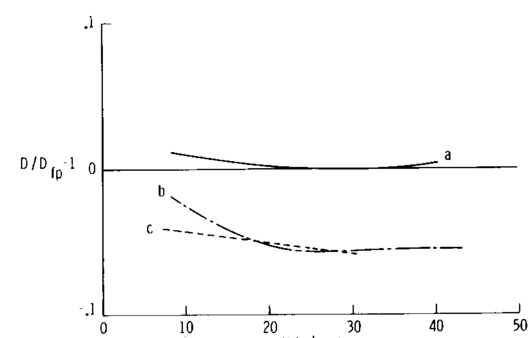

Figure 17 Direct drag for models C2: labels: a = base riblets alone, b = combined base and vinyl film riblets, c = vinyl film riblets alone

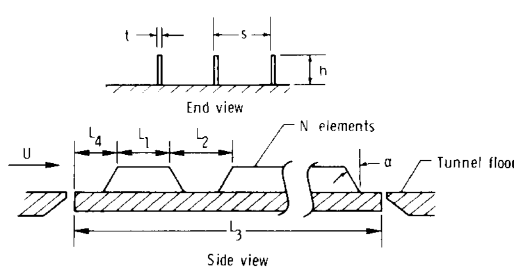

Figure 18 Three-dimensional riblet model 3D1: $s=0.69$, $h=0.51$, $t=0.051$, $L_1=8.38$, $L_2=6.32$, $L_3=304.8$, $L_4=8.54$, $\alpha=30°$, $N=20$ (all lengths in millimeters)

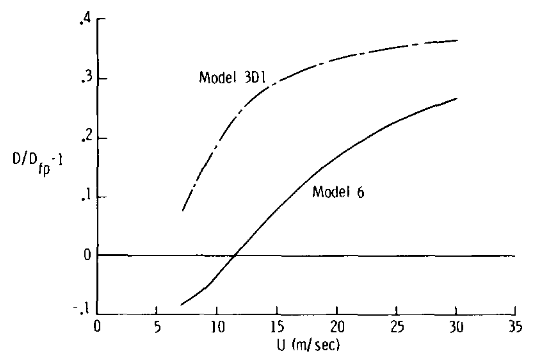

Figure 19 Direct drag for three-dimensional model 3D1 and two-dimensional model with same riblet height and spacing (Model 6, Table 1)

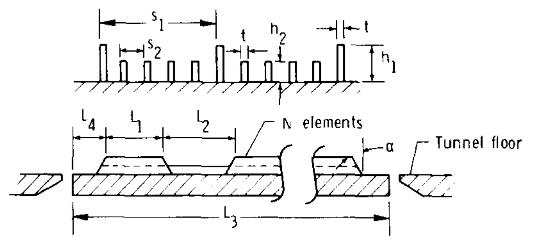

Figure 20 Three-dimensional model 3D2. $s_1=1.78$, $s_2=0.36$, $0.15<h_1<0.81$, $h_2=0.15$, $t=0.051$, $L_1=8.59$, $L_2=18$, $L_3=304.8$, $L_4=15.1$, $\alpha=60°$, $N=11$ (all lengths in millimeters)

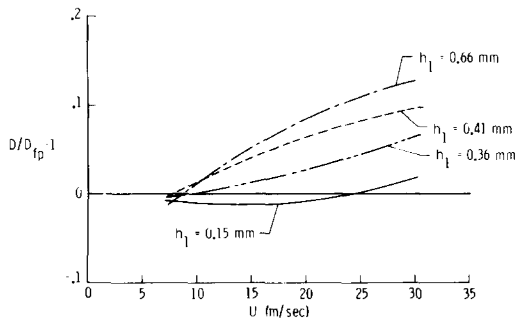

Figure 21 Direct drag for model 3D2 for various three-dimensional element heights (h_1)

increase in height of the three-dimensional riblet segments, indicating that the drag increase is largely due to increased wetted surface area.

Standby separation control for Stratford closure

Limited net drag benefits are available from tailoring of body adverse pressure gradient regions to induce local skin friction drag levels approaching zero over extended regions, the so-called Stratford closure. At subsonic speeds the direct skin friction benefits are partially offset by increased form or pressure drag due to decambering of the body. This decambering is caused by the increase in displacement thickness associated with more rapid boundary layer growth. Should separation occur huge pressure drag can obviously result, causing net drag increases. A possible further benefit from a Stratford-like pressure distribution is reduced structural weight, as the associated body closure is generally a local minimum weight solution. For supersonic flow the increased displacement thickness can actually be favorable, as the strength of the trailing edge shock, and therefore wave drag, is reduced.

In spite of the possible benefits, Stratford closures are not generally employed (except in some specialized airfoil designs) due to extreme off-design sensitivities. That is, any measurable deviation from the nearly zero skin friction design condition can result in large separated flow regions, attendant large drag increases, and possible controllability problems. A current research program at Langley attempts to address this off-design problem by conducting comparative studies, on the same canonical flow separation problem, of candidate *standby* flow separation control devices. The concept being that the Stratford design approach could be used if (preferably passive) flow separation control devices are utilized to treat the off-design case. Design requirements for such devices include minimum parasitic drag and weight and fail-safe operation. In the Langley research program in this area some 22 flow separation control approaches, many of them new, are applied to the same (initially quasi two-dimensional, later three-dimensional) separated flow to determine their relative efficacy in relation to the design requirements just described. As a minimum, this effort should yield alternative separated flow control devices for high lift, VSTOL, etc., applications.

Eddy substitution

The essentials of this approach involve substituting alternative flow modules for part of the usual turbulence motions. Once the substitution has occurred the modified flow can then be controlled in what is essentially a variant of the two-stage wall control discussed previously. Two efforts of this type are currently ongoing at Langley, one involving the outer flow and the other the near-wall flow. For the *outer flow case*, corotating longitudinal vortices are first generated relatively close together such that much of the outer turbulent boundary layer flow can be processed by the Rayleigh-stabilizing flow curvature induced by the three-dimensional vortex motion. Due to this stabilizing influence the center portion of a longitudinal vortex is generally a region of inordinately low turbulence. The vortex train is allowed to interact/alter the outer turbulence for the order of 20δ to 30δ to insure sufficient residence time for interactions to occur. Obviously during this period the mean entrainment into the boundary layer and the mean wall shear is increased by the macroscopic vortex motion. In the second stage vortex "unwinders," that is vortex generators of the opposite sense, are used to remove the control vortices and the modified boundary layer is allowed to relax, hopefully with a lower skin friction level. The unwinders should generate thrust, thereby partially offsetting the drag of the original vortex generators.

In the research thus far on this outer region eddy substitution and control device (a) the vortex unwinders have been shown to work extremely well, and (b) limited results suggest that the flow downstream of the unwinders has a reduced entrainment rate compared to the undisturbed case.[50] As a spinoff from this research the unwinders have been employed for direct vortex control in intersection regions such as submarine sail/hull interactions. In the current research seven-hole probes are employed to obtain improved diagnostics of the relaxation process.

The *near wall* eddy-substitution approach involves the use of small transverse cavities with length-to-depth ratios of order 1 (to avoid reattachment within the cavity) and order of 50 wall units in size (to avoid embedded shear-layer instabilities). In the absence of turbulence the innate drag of such surfaces is low; the presence of near-wall turbulence causes random "eruption" of low momentum fluid from the cavities and attendant "pulses" of increased pressure drag which aggregates to an elevated net drag level.[51,52] Limited data indicate the Reynolds stress over such surfaces is reduced compared to a smooth surface (see Ref. 1). Langley is currently pursuing two approaches for control/reduction of the wall eruptions from small transverse cavities. The first approach is quite simple and consists merely of utilizing *near wall* longitudinal vortex generators to substitute quasistationary vortices (corotating) for the usual turbulence chaos near the wall and thereby protect the cavities from part of the turbulence-induced pressure fields responsible for the cavity eruptions. The second approach entails excitation of a coherent Stokes flow in the cavity and the subsequent control of this motion,[53] the thought being that if you cannot easily control what exists naturally then substitute a flow that you *can* control.

Relaxation from wall curvature effects

As is well known, the influence of convex longitudinal curvature upon turbulent boundary layer structure is similar to that of large-eddy breakup devices only more extreme (for small radius of curvature positive Reynolds stresses can be produced in the outer flow!). The outer motions are damped thereby reducing the wall shear. Since the local effects are similar to LEBU devices the relaxation behavior should be also and the basic concept for this approach is to utilize convex wall curvature in place of a LEBU. (What is just being sorted out is that "in-plane" curvature (streamline curvature in the xz or body surface plane) can also provide appreciable damping to the turbulence structure, e.g., Ref. 54.) The limited curvature relaxation studies available thus far indicate diverse behavior. In some of the works the curvature is not applied to the flow for a long enough distance to fully alter the turbulence and therefore the observed relaxation is probably too rapid. In other cases the local pressure gradients (or lack thereof) allow the local mean shear to become so large that appreciable additional turbulence production occurs. Therefore current nominal design requirements for this turbulent drag reduction approach include (a) large δ/R (order of 0.05 to 0.1), (b) $\Delta x/\delta$ (spatial extent of the flow affected by the curvature) order of 15 or greater, and (c) local favorable pressure gradient to keep the mean shear low in the mid region of the boundary and new turbulence production reduced. The model configurations employed in this research for both subsonic and supersonic flows are shown in Ref. 1. What is particularly intriguing is the possibility of using this approach for the supersonic case, where large device wave drag would normally obviate the use of large-eddy breakup devices. A variant of this approach involved study of "waisted" axisymmetric bodies where computations suggest a net reduction of between 5% and 10% due to the combined effect of convex curvature and adverse pressure gradient.[55]

Approaches which evidently do not work

The NASA Langley Turbulent Drag Reduction Program has been structured with a conscious attempt to be innovative and inventive, the sheer size and importance of the payoff providing the justification for pursuing any nonridiculous possibility. Studies indicate that the essence of innovative research is often a failure; a success rate of the order of 10 to 20% in truly inventive work is considered superlative. The present section of the report is included in the interests of completeness and in the hope that the discussions will provide insights to move the field forward and build upon what has already been done.

Wall waviness

Three types of wall waviness were examined, two stationary and the other dynamic. Fixed transverse waves, which provide alternating regions of longitudinal concave and convex curvature along with alternating adverse and favorable pressure gradients were studied to a considerable extent, both experimentally and numerically (e.g., Ref. 56). What was intriguing was the initial observations that, for wavelengths approaching the boundary layer thickness, the coincidence of convex curvature and favorable pressure gradient appeared to cause periodic partial relaminarization. Data indicated average skin friction reductions of 10 to 20%. The problem was the attendant phase shift in the wall pressure field which caused "device" pressure drag in excess of this net skin friction reduction. The Langley program sought to understand the physics of the wavy-wall flow and to design nonsinusoidal surfaces which might retain the skin friction reduction but exhibit less pressure drag. The effort was successful to the extent that the skewed waves did have lower pressure drag but the best surfaces developed only produced net reductions (including the area increase) of 1 to 2%, hardly worth pursuing further.

The other fixed wall waviness involved waves with axis aligned with the flow, providing oscillatory transverse curvature. These were essentially large scale riblets, with dimensions the order of the boundary layer thickness. Limited data indicate that sufficiently small (external flow) transverse curvature will cause relaminarization, while curvature of the opposite sign thickens the boundary layer and reduces mean shear. Parametric models were tested and the results indicate net drag increases, but with an intriguing trend toward lower drag increases at high Reynolds number. The method was not deemed to be sufficiently promising to merit further research and was dropped, but studies of the turbulence structure of flow-aligned waviness over a wide parameter range should probably be carried forward, if only for application to structural stiffeners and heat exchangers.

The dynamic wall waviness investigated involved various forms of the compliant wall concept. The early Langley work on passive compliant wall was quite extensive and concluded with a summary document (Ref. 2 and refs. therein). Many types of surfaces were employed (including driven walls),[57] but the major contribution of the work was to provide alternate explanations for many of the previously apparently "successful" studies. The conclusion was that, for turbulent boundary layers in air, evidently compliant wall drag reduction was "a subject without an object." More recently phase-locked wall motion was tried in an attempt to obviate the burst-producing instantaneous wall region connected adverse pressure gradients.[58] The build-up of such a region was first sensed and then the wall was magnetically deflected down and the wave convected downstream in phase with, and at the dimensions of, the dynamic motions responsible for initiating wall bursting. The effort was heroic and successful to the extent that dynamic adverse pressure gradients in the wall region could be "canceled." However, the effort was conducted at low speeds and was discontinued due to the same reason there are no 3000-lb birds: inertia scaling problems. We could not envisage a technique to make such phase-locked interactive walls work at the scales and frequencies associated with near-transonic flight. The sensors and computing power is at hand for intelligent walls, but the requisite "effectors" or actuators are not, at least for the air case.

Injection

Several injection techniques were attempted, utilizing a wide variety of injectants. In fact one of these, slot (wall wake) tangential injection utilizing LFC suction air and LEBUs to reduce "free mixing" between the injected and external flows is still on the "active" list (see earlier LEBU discussion in present paper). However, several other injection schemes did not fare as well. An early (circa 1978) in-house injection study addressed the concept of using particles/fibers to reduce fuselage skin friction. Long thin particles reduce skin friction in air and the concept was to inject these particles behind the cockpit, accrue drag reduction along the fuselage and then collect them at the rear for recycling. The problem with this approach was the unrealistically large collection efficiency required. In view of this an obvious variant was to utilize solid fuel and inject it, taking the fuel into the propulsion system through a boundary-layer inlet at the rear (after the fuel had reduced the fuselage drag). This particular approach was deemed more of a systems problem than anything else and was never actively pursued. A variant of this variant was to inject gaseous fuel in essentially a slot injection (low momentum wall wake) scenario[59] with subsequent collection in a boundary-layer inlet at the rear. This approach floundered due to the small fuel flow rate compared to the boundary-layer mass flow; i.e., the low drag region was of quite limited extent. Porous wall (normal) injection was never seriously studied in the Langley program due to the extensive literature already available and the success of turbulence modeling and CFD techniques in handling this case. Porous wall injection will in fact provide large skin friction reductions, and provides an alternative to slot injection if a low-loss source of injectant, such as LFC suction air, is available.

Direct wall region momentum reduction

Various attempts were made to reduce the wall region longitudinal momentum more or less directly. Considerable effort was expended studying the "ion wind."[60] Aircraft charge to the order of 3×10^5 volts and this is currently dissipated to avoid interference with communications and reduce the risk of explosions, etc. The idea was to promote, using this source, a corona discharge from small (subroughness) wall electrodes, thereby setting up an "ion wind." This would utilize electrostatic body forces to convert longitudinal into vertical motion near the wall, providing the advantages (low drag) of wall blowing without the need for actual mass transfer through the wall. Both theory and experiment indicated sizable skin friction reductions but the method is only suitable for low speeds. At the higher velocity the corona is not as efficient and the velocities produced are not large enough to provide sizable drag reductions at high speeds.

Restriction to low-speed operation is also a problem with another technique briefly examined—wall cooling. Sufficient wall cooling can, in air through turbulence stabilization, reduce turbulent drag significantly, but reasonable cooling restricts the approach to ultra low velocities.[1] Heating the wall (in air) reduces the wall momentum directly and various sums were run out using conventional turbulence modeling.[61] However, the particular application of this obvious approach is limited to situations where large amounts of waste heat are available, certainly not the case for aircraft.

In another attempt to reduce the mean near-wall longitudinal momentum, the Lobert concept[62] of an upstream wind turbine to reduce the near-body momentum combined with a through-body shaft and a propulsor at the rear was studied. The results indicate major sensitivities to component efficiencies and an unknown degradation due to turbulence/skin friction increases from the turbine tip vortex-body interaction.[63] Again, this was viewed as (a) not having spectacular benefits, and (b) more of a system than a fluid dynamic problem and therefore dropped.

Turbulence control

Several other techniques aimed at altering the turbulence structure were also tried (along with riblets, LEBUs, two-stage control and the phase-locked wall motion already discussed). One of these approaches has enjoyed rather spectacular success, but not for turbulent drag reduction. The basic idea was to test a passive porous wall, i.e., to obviate the $v \cdot n = 0$ wall-boundary condition but allow no net mass transfer. This was tried at hypersonic speeds at Langley with null results[64] and was retried at low speeds more recently with an equally disappointing outcome[65]. However, such a wall was suggested by Langley (in conjunction with a subsurface plenum) to Nagamatsu in the late 1970s as a method of passively controlling separation in shock-boundary layer interactions and his research (Ref. 66 and subsequent works), along with that of the West Germans indicate that the method is particularly well suited as a standby separation and wave-drag reduction device for thick supercritical ("shockless") wings at off-design conditions.

A somewhat similar type of "absorbing wall" was also tried to alter vortex-wall interactions, which are evidently some of the more important physical processes associated with turbulence production. Longitudinal grooves and "strings" of various types and arrangements, both on and in the vicinity of the surface were tried—many reminiscent of the early Kramer patent. The results of all of this research were net drag increases, as were studies of "near-wall" vortex generators to replace the turbulence with a deterministic flow.[67] One reason for the failure of devices employing streamwise "strings" such as in the Kramer patent is the large increase in C_f on the strings due to convex curvature.

Another attempt at direct turbulence control involved the dynamic production of Emmons spots at high frequency and closely spaced spanwise to force nearly instant transition and to produce small outer scales initially rather than let the natural large ones develop and then alter them with LEBUs, etc. The technique worked; the downstream drag was reduced by approximately the same amount as a LEBU if one subtracts from the LEBU results the effect of the device momentum deficit.[68] Unfortunately, the energy required to force the Emmons spots was much larger than the integrated drag reduction and therefore the method was dropped.

Attempts were also made to produce "negative" dynamic vorticity. The simplest idea was that much of the turbulent dynamic vorticity has the same sign as the mean vorticity and therefore if dynamic vorticity of the opposite sign could be produced in the boundary layer some "favorable" (turbulence damping) interaction might occur.Three techniques were tried (a) a flow-turned Sevonius rotor, (b) a transverse cylinder with a control plate mounted above it to force a "one-sided" Karman street, and (c) various short protuberances mounted upside down on a LEBU to produce "negative horseshoes." In the first approach the rotor did not turn fast enough and led to a rule-of-thumb for the Langley program: "If the technique involves moving solid bodies in general it either will not work or cannot be scaled up to transonic speeds." The second approach produced the requisite negative dynamic vorticity which did have a measurable favorable effect on the turbulence, but the device drag was, understandably, tremendous.[69,70] The third approach has been difficult to implement and thus far has yielded little.

Conclusions

1. Conventional riblets work even in the presence of reasonable flow inclination and pressure gradients and at transonic

speeds, and are in the final stages of application research with the major issues being porosity implementation and particle adhesion during flight.
2. Nonconventional riblet research (alternative mechanisms, compound geometries) indicate improved turbulence alteration and performance at higher wavelength but no increase in net drag reduction.
3. The variability in LEBU results from laboratory-to-laboratory and even within the same laboratory is ascribed to the inordinately low device chord Reynolds numbers associated with university-scale low-speed facilities. Results at (higher) flight-device chord Reynolds numbers are expected to be less spectacular than the best existing results (due to turbulent device drag) but much more repeatable. The expected net benefit is in the 8 to 15% range depending upon the performance of a single device at high Reynolds number. For near transonic flight application the nontrivial problems of device stiffness and wave drag reduction have yet to be definitively solved.
4. Among the multitudinous alternative approaches under study, the two-stage approach is the most interesting but early results are not encouraging.
5. There are many important alternative applications for this turbulence control research besides drag reduction including (a) heat transfer augmentation at constant pumping power,[26] (b) self-noise reduction,[71] (c) reduction of turboprop-fuselage noise interaction, (d) free-mixing control,[72] (e) flow-separation control through turbulence augmentation, and (f) sensor performance improvements.

References

1 Bushnell, D. M. Turbulent Drag Reduction for External Flows. Aircraft Drag Prediction and Reduction, AGARD Report 723, 1985

2 Bushnell, D. M., Hefner, J. N. and Ash, R. L. Effect of Compliant Wall Motion on Turbulent Boundary Layers. Special Course on Concepts for Drag Reducton, AGARD R-654, Mar 1977

3 Walsh, M. J. Drag Characteristics of V-Groove and Transverse Curvature Riblets. *Viscous flow drag reduction*, Progress in Astronautics and Aeronautics, 1980, Vol. 72, 168–184

4 Hefner, J. N., Weinstein, L. M., and Bushnell, D. M. Large-Eddy Breakup Scheme for Turbulent Viscous Drag Reduction. *Viscous flow drag reduction*, Progress in Astronautics and Aeronautics, 1980, Vol. 72, 110–127

5 Corke, T. C., Guezennec, Y., and Nagib, H. M. Modification in Drag of Turbulent Boundary Layers Resulting from Manipulation of Large-Scale Structures. *Viscous flow drag reduction*, Progress in Astronautics and Aeronautics, 1980, Vol. 72, 128–143

6 Walsh, M. J. Turbulent boundary layer drag reduction using riblets. *AIAA Paper* No. 82-0169, Jan 1982

7 Walsh, M. J. Optimization and application of riblets for turbulent drag reduction. *AIAA Paper* No. 84-0347, Jan 1984

8 Walsh, M. J. and Weinstein, L. M. Drag and heat transfer on surfaces with small longitudinal fins. AIAA Eleventh Fluid and Plasma Dynamics Conference, Seattle, Washington, July 11–12, 1978, *AIAA Paper* No. 78-1161

9 Walsh, M. J. and Weinstein, L. M. Drag and heat transfer characteristics of small longitudinally ribbed surfaces. *AIAA J.*, **17**(7), July 1979

10 Bechert, D. W., Bartenwerfer, M., Hoppe, G., and Reif, W. E. Drag Reduction Mechanisms Derived from Shark Skin. Paper No. 86–1.8.3. Presented at Fifteenth Congress, International Council of the Aeronautical Sciences London, Sept 1986

11 Bechert, D. W., Hoppe, G., and Reif, W.-E. On the drag reduction of the shark skin. *AIAA Paper* No. 85-0546, Mar 1985

12 Nitschke, P. Experimental investigation of turbulent flow in smooth and longitudinal grooved tubes, NASA TM–77480, May 1984

13 Nagel, A. L., George-Falvy, D., and McLean, J. D. Riblet flight tests on a small airplane. Abstract, Drag Reduction and Boundary Layer Control Symposium, National Academy of Sciences, Washington, DC, Oct 1985

14 Hooshmand, A., Youngs, R. A., Wallace, J. M., and Balint, J. L. An experimental study of changes in the structure of a turbulent boundary layer due to surface geometry changes. *AIAA Paper* No. 83-0320, 1983

15 Gallagher, J. A. and Thomas, A. S. W. Turbulent boundary layer characteristics over streamwise grooves. *AIAA Paper* No. 84-2185, Aug 1984

16 Eilers, R. E., Koper, C. A., McLean, J. D., and Coder, D. W. An Applicaton of Riblets for Turbulent Skin-Friction Reduction. *Twelfth Symposium on Sailing*, AIAA and Univ. of Washington, Seattle, Sept 1985

17 Khalid, M. An Experimental Investigation of Skin Friction on Smooth Surfaces Supporting Air Bearing Channels. NAE-AN-391, NRC No. 26163, National Aeronautical Establishment, Ottowa, July 1986

18 Chen, J. J. J., Leung, Y.-C., and Ko, N. W. M. Drag reduction in a longitudinally grooved flow channel. *Ind. Eng. Chem. Fundam.*, 1986, **25**

19 Sawyer, W. G. and Winter, K. G. The effect on turbulent skin friction of surfaces with streamwise grooves. Abstract, European Meeting on Turbulent Drag Reduction, Lausanne, Sept 1986

20 Coustols, E., Cousteix, J., and Dickinson, J. Turbulent boundary layer characteristics and drag reduction due to surface geometry changes: "riblets". Abstract, European Meeting on Turbulent Drag Reduction, Lausanne, Sept 1986

21 Savill, A. M. and Squire, L. C. High speed riblets. Abstract, European Meeting on Turbulent Drag Reduction, Lausanne, Sept 1986

22 Reidy, L. W. V-Groove Surface Modifications in a Turbulent Boundary Layer for High-Speed Water Flow. Naval Ocean Systems Center, Tech Note 1444, San Diego, CA, Mar 1986

23 Bacher, E. V. and Smith, C. R. A combined visualization-anemometry study of the turbulent drag reducing mechanisms of triangular micro-groove surface modifications. *AIAA Paper* No. 85-0548, Mar 1985

24 Wilkinson, S. P. and Lazos, B. S. Direct Drag and Hot-Wire Measurements on Thin-Element Riblet Arrays. IUTAM Symposium on Turbulence Management and Relaminarization, Bangalore, Jan 1987

25 Walsh, M. J. and Anders, J. B. Riblets Optimized for Flight Application. Abstract, Drag Reduction and Boundary-Layer Control Symposium, National Academy of Sciences, Washington, DC, Oct 1985

26 Lindemann, A. M. Turbulent Reynolds analogy factors for nonplanar surface microgeometries. *J. Spacecraft and Rockets*, September–October 1985, **22**(5), 581–582

27 Choi, K.-S. The Wall Pressure Fluctuations of Modified Turbulent Boundary Layer With Riblets. IUTAM Symposium on Turbulence Management and Relaminarization, Bangalore, Jan 1987

28 Falco, R. E. Experimental Investigation of the Turbulence Production Mechanism in Boundary Layers. AFOSR-TR-86-0942 Report, Aug 1986

29 Khan, M. M. S. A numerical investigation of the drag reduction by riblet surfaces. *AIAA Paper* No. 86-1127, May 1986

30 Sandborn, V. A. and Chen Chion, H. A Model for and Techniques of Modifying the Surface Shear Fluctuations in a Turbulent Boundary Layer. *Proceedings of the Seventh Symposium on Turbulence*, University of Missouri-Rolla, 1983

31 Liu, C. K., Kline, S. J., and Johnston, J. P. An Experimental Study of Turbulent Boundary Layer on Rough Walls. Stanford University, Dept. Mech. Eng., Report MD-15, July 1966

32 Nakagawa, H. and Nezu, I. Coherent Structures in Open Channel Flow, in *Structure of Turbulence in Heat and Mass Transfer*, ed. Z. P. Zariv, Hemisphere Publishing Company, Washington, 1982

33 Yajnik, K. S. and Ancharya, M. Nonequilibrium Effects in a Turbulent Boundary Layer Due to the Destruction of Large Eddies. National Aeronautical Lab, Bangalore, NAL-BL-7, Aug 1977

34 Corke, T. C., Guezennec, Y., and Nagib, H. M. Modifications

of Drag of Turbulent Boundary Layers Resulting From Manipulation of Large-Scale Structures. Symposium on Viscous Drag Reduction, Dallas, Texas, Nov 7–8, 1979

35 Corke, T. C., Guezennec, Y., and Nagib, H. M. Modifications of drag of turbulent boundary layers resulting from manipulation of large-scale structures, NASA CR-3444, July 1981

36 Corke, T. C., Nagib, H. M., and Guezennec, Y. A new view on origin role and manipulation of large scales in turbulent boundary layers, NASA CR-165861, Feb 1982

37 Hefner, J. N., Weinstein, L. M., and Bushnell, D. M. Large-Eddy Breakup Scheme for Turbulent Viscous Drag Reduction. Symposium on Viscous Drag Reduction, Dallas, Texas, November 7–8, 1979

38 Hefner, J. N., Anders, J. B., and Bushnell, D. M. Alteration of outer flow structures for turbulent drag reduction. *AIAA Paper* No. 83-0293, Jan 1983

39 Anders, J. B., Hefner, J. N., and Bushnell, D. M. Performance of large-eddy breakup devices at post-transitional Reynolds numbers. *AIAA Paper* No. 84-0345, Jan 1984

40 Bushnell, D. M. Turbulent drag reduction for external flows. *AIAA Paper* No. 83-0227, Jan 1983

41 Anders, J. B. and Watson, R. D. Airfoil large-eddy breakup devices for turbulent drag reduction. *AIAA Paper* No. 85-0520, Mar 1985

42 Anders, John B. Large-eddy breakup devices as low Reynolds number airfoils. Presented at the SAE Aerospace Technology Conference and Exposition, Long Beach, California, Oct. 13–16, 1986. *SAE Paper* No. 86-1769

43 Mueller, T. J., Pohlen, L. J., Conigliaro, P. E., and Jansen, B. J. The influence of free-stream disturbances on low Reynolds number airfoil experiments. *Experiments in Fluids*, 1985, **1**, 3–14

44 Lissaman, P. B. S. Low-Reynolds Number Airfoils. Annual Reviews of Fluid Mechanics, 1983

45 Mueller, T. J. Aerodynamic measurements at low Reynolds numbers. *AIAA Paper* No. 82-0598, Mar 1983

46 Papathanaslou, A. G. and Nagel, R. T. Boundary-layer control by acoustic excitation. *AIAA Paper* No. 86-1954, 1986

47 Balakumar, P. and Widnall, S. E. Application of unsteady aerodynamics to large-eddy breakup devices in a turbulent flow. *Physics of Fluids*, June 1986, **29**(6)

48 Bertelrud, Arild. Full Scale Experiments into the Use of Large-Eddy Breakup Devices for Drag Reduction on Aircraft. AGARD Symposium on Improvement of Aerodynamics Performance Through Boundary-Layer Control and High Lift Systems. AGARD Conference Proceedings No. 365, May 1984

49 Gad-el-Hak, M. and Blackwelder, R. F. A drag reduction method for turbulent boundary layers. *AIAA Paper* No. 87-0358, Jan 1987

50 McGinley, C. B. and Beeler, G. B. Large-eddy substitution via vortex cancellation for wall turbulence control. AIAA Shear Flow Control Conference, Mar 12–14, Boulder, CO, *AIAA Paper* No. 85-0549

51 Gatski, T. B. and Grosch, C. E. Embedded cavity drag in steady and unsteady flows. Presented at the AIAA 22nd Aerospace Sciences Meeting, Reno, NV, Jan 9–12, 1984. *AIAA Paper* No. 84-0436

52 Gatski, T. B. Drag characteristics of unsteady, perturbed boundary flows. Presented at the AIAA Shear Flow Control Conference, Boulder, CO, March 12–14, 1985. *AIAA Paper* No. 85-0551

53 Bandyopadhyay, P. R. Resonant flow in a row of small transverse cavities submerged in a turbulent boundary layer. Presented at the AIAA 19th Fluid Dynamics, Plasma Dynamics and Laser Conference, Honolulu, Hawaii, June 8–10, 1987. *AIAA Paper* No. 87-1235

54 Bradshaw, P. and Pontikos, N. S. Measurements in the turbulent boundary layer on an "infinite" swept wing. *J. Fluid Mech.*, 1985, **159**, 105–130

55 Lin, John C., Weinstein, L. M., Watson, R. D., and Balasubramanian, R. Turbulent drag characteristic of small amplitude rigid waves. Presented at the AIAA 21st Aerospace Sciences Meeting, Reno, NV, Jan 10–13, 1983. *AIAA Paper* No. 83-228

56 Lin, John C., Walsh, Michael J., and Balasubramanian, R. Drag of two-dimensional small-amplitude symmetric and asymmetric wavy walls in turbulent boundary layers. NASA TP-2318, June 1984

57 Weinstein, L. M. Effect of driven-wall motion on a turbulent boundary layer. Unsteady turbulent shear flows, IUTAM Symposium, Toulouse, France, 1981

58 Wilkinson, S. P. and Balasubramanian, R. Turbulence burst control through phase-locked traveling surface depressions. AIAA Shear Flow Control Conference, Boulder, CO, Mar 12–14, 1985. *AIAA Paper* No. 85-0536

59 Cary, A. M., Jr., Bushnell, D. M., and Hefner, J. N. Slot Injection for Skin-Friction Drag Reduction. Special Course on Concepts for Drag Reduction, AGARD R-654, Mar 1977

60 Malik, M. R., Weinstein, L. M., and Hussaini, M. Y. Ion wind drag reduction. Presented at the AIAA 21st Aerospace Sciences Meeting, Reno, NV, Jan 10–13, 1983. *AIAA Paper* No. 83-0231

61 Lin, J. C. and Ash, R. L. Wall Temperature Control of Low-Speed Body Drag. *J. Aircraft*, Jan 1986, **23**(1), 93–94

62 Lobert, G. Drag Reduction by Means of Active Boundary Layer Thickening. Israel Annual Conference on Aviation and Astronautics, 23rd Tel Aviv and Haifa, Israel, Feb 11–12, 1981, 236–242

63 Ash, R. L. An investigation of the feasibility of active boundary layer thickening for aircraft drag reduction. NASA CR-177133, Apr 1986

64 Watson, Ralph D. Exploratory investigation of the effect of porous surfaces on hypersonic turbulent boundary layers. NASA TM 78791, Jan 1979

65 Wilkinson, S. P. Influence of wall permeability on turbulent boundary-layer properties. AIAA 21st Aerospace Sciences Meeting, Reno, NV, Jan 10–13, 1983. *AIAA Paper* No. 83-0294

66 Bahi, L., Ross, J. M., and Nagamatsu, H. T. Passive shock wave/boundary layer control for transonic airfoil drag reduction. *AIAA Paper* No. 83-0137, Jan 1983

67 Rao, D. M. and Mehrotra, S. C. Flat-plate drag measurements with vortex generators in turbulent boundary layer. NASA CR-172125, June 1983

68 Goodman, W. L. Emmons Spot Forcing for Turbulent Drag Reduction. *AIAA J.*, Jan 1985, **23**(1), 155–157

69 Goodman, W. L. The effect of opposing-unsteady vorticity on the turbulent structures in wall flow. AIAA Shear Flow Control Conference, Boulder, CO, Mar 12–14, 1985. *AIAA Paper* No. 85-0550

70 Goodman, W. L. Modification of the Karman-vortex street in the freestream. *AIAA J.*, Sept 1986, **24**(9), 1556–1557

71 Beeler, G. B. Turbulent boundary-layer wall pressure fluctuations downstream of a tandem LEBU. *AIAA J.*, Apr 1986, **24**(4), 689–691

72 McInville, R. M. Numerical and Experimental Investigation of Forced Laminar Free Shear Layers and Turbulent Slot Injection Flows. Ph.D. Dissertation, North Carolina State University, 1985